Three-dimensional Augmented Reality-guided Robotic-assisted Kidney Transplantation: Breaking the Limit of Atheromatic Plaques

This is a postprint version of the article published in *European Urology*

The final published article is available online at https:doi.org

https://doi.org/10.1016/j.eururo.2022.07.003

Cite this article as

Alberto Piana, Andrea Gallioli, Daniele Amparore, Pietro Diana, Angelo Territo, Riccardo Campi, Josep Maria Gaya, Lluis Guirado, Enrico Checcucci, Andrea Bellin, Joan Palou, Sergio Serni, Francesco Porpiglia, Alberto Breda; Three-dimensional Augmented Reality-guided Robotic-assisted Kidney Transplantation: Breaking the Limit of Atheromatic Plaques. Autocrine 17-β-Estradiol/Estrogen Receptor-α Loop Determines the Response to Immune Checkpoint Inhibitors in Non-Small Cell Lung Cancer. Eur Urol. 2022 Oct;82(4):419-426

Three-dimensional Augmented Reality-guided Robotic-assisted Kidney Transplantation: Breaking the Limit of Atheromatic Plaques

Alberto Piana[1], Andrea Gallioli[2], Daniele Amparore[3], Pietro Diana[2], Angelo Territo[2], Riccardo Campi[4], Josep Maria Gaya[2], Lluis Guirado[5], Enrico Checcucci[3], Andrea Bellin[3], Joan Palou[2], Sergio Serni[4], Francesco Porpiglia[3], Alberto Breda[2]

Affiliations

1 Department of Urology, Fundació Puigvert, Autonomous University of Barcelona, Barcelona, Spain; Department of Urology, "San Luigi Gonzaga" Hospital, University of Turin, Turin, Italy. Electronic address: alb.piana@gmail.com.

2 Department of Urology, Fundació Puigvert, Autonomous University of Barcelona, Barcelona, Spain.

3 Department of Urology, "San Luigi Gonzaga" Hospital, University of Turin, Turin, Italy.

4 Department of Urology, Careggi Hospital, University of Florence, Florence, Italy.

5 Department of Nephrology, Fundació Puigvert, Autonomous University of Barcelona, Barcelona, Spain.

Abstract

Background

Robotic-assisted kidney transplantation (RAKT) has shown solid results as a minimally invasive alternative to the standard open approach (open kidney transplantation [OKT]). However, RAKT is still limited in those cases where the recipient’s iliac vessels present atherosclerotic plaques, frequently found in elder patients and in those subjected to long-term hemodialysis. Unlike OKT, where the surgeon can palpate the arterial plaques, in minimally invasive surgery the haptic feedback is missing, making the vascular clamping and arteriotomy unsafe.

Objective

To employ three-dimensional (3D) imaging reconstruction using augmented reality (AR) to intraoperatively locate the plaques during the crucial steps of kidney transplantation.

Design, setting, and participants

Our study was conducted according to the Idea, Development, Exploration, Assessment, and Long-term follow-up (IDEAL) model for surgical innovation. Three-dimensional virtual models were obtained from high-accuracy computed tomography scan imaging and superimposed on the vessels during RAKT using the Da Vinci console software.

Surgical procedure

Three-dimensional AR–guided robotic-assisted kidney transplantation.

Measurements

The correspondence of virtual models with the real anatomy of patients was assessed comparing vessels' and plaques' measures.

Results and limitations

We tested the possibility of using the AR in the setting of vascular surgery by checking the correspondence of the virtual models to the real vessels. During the accuracy assessment, we investigated the anatomy of the iliac plaques and the capacity of the virtual models to correctly represent them. Finally, we tested the efficacy of the virtual model superimposition on the real vessels with plaques during RAKT in the recipients of living donor grafts. The main limitation consists in training needed to correctly superimpose virtual models on the real field.

Conclusions

The employment of 3D AR allowed surgeons to overcome one of the main limitations of RAKT, setting the foundation to expand its indications to patients with advanced atheromatic vascular disease.

Patient summary

The use of three-dimensional augmented reality guidance during kidney transplantation (KT) has the potential to "navigate" the surgeon during KT, allowing a safer procedure in patients with atheromatic vascular disease.

1. Introduction

Kidney transplantation (KT) is the best replacement treatment for end-stage renal disease (ESRD) [1], [2]. The open approach (open KT [OKT]) is still considered the gold standard treatment in KT, despite the high rate of morbidity and its surgical invasiveness [3]. Robotic-assisted kidney transplantation (RAKT) has been proposed as a valid minimally invasive alternative to OKT for a living donor's KT [4], [5].

However, RAKT is still limited in those cases where the recipient's iliac vessels present atherosclerotic plaques, a frequent finding in elderly patients and in those subjected to long-term hemodialysis. Unlike OKT, where the surgeon can manually palpate the arterial plaques, in minimally invasive surgery, the haptic feedback is missing, making the vascular clamping and arteriotomy unsafe.

To overcome this limit, three-dimensional (3D) imaging virtual reconstruction was employed through the augmented reality (AR) in RAKT to intraoperatively locate the arterial plaques and drive the surgeon during

the crucial steps of the procedure. The use of this technology has already shown outstanding results, driving the surgeon during oncological surgery to improve the outcomes [6].

In this multistep project, we employed 3D AR with the aim of expanding the role of RAKT in patients with severe atheromatic vascular disease.

2. Patients and methods

2.1. Study design and population

This is a prospective study developed according to the Idea, Development, Exploration, Assessment and Long-term follow-up (IDEAL) [7] model for surgical innovation. Phase 0 of this study was already described [8].

In phase 1, 3D printed and virtual models of recipients' common and external iliac arteries with atheromatic plaques were obtained from high-accuracy conventional noncontrast computed tomography (CT) scan imaging. The acquisition of the CT images was performed by an expert radiologist, and the virtual reconstruction of the iliac vessels was performed by bioengineers from Medics (Turin) guided by expert urologists to verify the accuracy of the anatomical representation. Virtual reconstruction of other anatomical pelvic structures (ie, ureters) to be used as landmarks for an easier overlap was eventually realized after a case-by-case evaluation. Finally, the virtual reconstruction was superimposed through the AR technology on the real anatomy of the patients during RAKT using the Da Vinci console software.

From October 2020 to October 2021, 19 patients were enrolled in this study. The inclusion criteria were patients ≥18 yr old with ESRD and an American Society of Anesthesiologists score of ≤3.

The study has been divided into three steps: feasibility, accuracy, and efficacy assessment. The endpoint of the first step was to describe the feasibility of the superimposition of 3D virtual models on the real vessels to assess their fidelity in a safe setting without arterial plaques. The second step of the project tested the accuracy of virtual models' superimposition on the iliac vessels during robot-assisted pelvic lymphadenectomy in patients with iliac plaques submitted to radical prostatectomy and thus not candidate for vascular surgery. Finally, the objective of the third step was to assess the efficacy of the procedure during RAKT, evaluating its role in clinical cases of recipients of a living donor graft with iliac artery plaques.

2.2. Feasibility assessment

The aim of this step was to demonstrate the possibility of using the 3D AR in the setting of vascular surgery by checking the correspondence of the virtual models to the real vessels. The first issue was to find anatomical landmarks to allow a precise superimposition of the virtual models. The correct assessment of the orientation of the vessel and the rotation on its axes is crucial in this phase. A minimal error in the orientation and/or rotation of the vessel may lead to significant subsequent discordance in the representation of the plaques and, thus, to a significant risk of unsafe clamping and arteriotomy. For this reason, anatomical landmarks were mandatory to assure correct positioning of the 3D model. The following landmarks were employed: common iliac bifurcation and eventual crossing ureter (Fig. 1). At this point, virtual ring markers were designed in the external iliac virtual artery model at a distance of 1 cm from each other, to allow a virtual measurement of the vessel. The iliac vessel circumference was measured on CT scan images just above the hypogastric artery ramification, at the level of the major plaque and at the level of lacuna vasorum. Each real vessel size at this level was compared with the virtual model to assess reconstruction fidelity.

2.3. Accuracy assessment

The second step was to investigate the anatomy of the iliac plaques and the capacity of the virtual models to correctly represent/locate them. We considered for this phase a setting of patients in whom the

exposure of the anatomical structures is similar to the one of the transplant but in whom the presence of arterial plaques is most frequent, such as for patients undergoing robot-assisted radical prostatectomy with pelvic lymphadenectomy. For this cluster of patients, the superimposition of the virtual image on the real iliac artery was performed after their exposure during pelvic lymphadenectomy. An ultrasound (US) drop-in probe was used on the dissected iliac vessel surface while the 3D model of the plaques was superimposed. In order to evaluate the extent of the plaque, the robotic probe was orientated perpendicularly to the external iliac vessel of interest and slid from its origin to the last level of its permanence in the pelvic space (identified as the point of its passage in the vascular lacuna). The correspondence of the longitudinal and transverse edges of the virtual reconstruction of the hidden plaques was verified (Fig. 2) and measured with the US probe (Fig. 3).

2.4. Efficacy assessment

The final step was to test the efficacy of the virtual model superimposition on the real vessels with plaques during RAKT in recipients of the living donors' grafts. The superimposition was performed after partial isolation of the vessel, which allowed an adequate medial exposure of the artery without affecting in any way the local anatomy represented in the model. In fact, a complete dissection of the vessel would slightly change the position of the vessel itself in the pelvis, thus modifying the fidelity of a virtual model created from a static CT scan imaging.

At this point, the anatomical landmarks were identified and the superimposition of the model is realized. To confirm the position of the plaques, a US artery scan was performed with a robotic drop-in probe. Then, the vessel was gently marked on its surface with superficial monopolar burns to delimitate the operative surface. Finally, the clamps were placed and the arteriotomy was realized (Fig. 4).

A safe clamping, defined as a complete and bloodless closure of the vascular bulldog, was always verified.

2.5. Ethical approval

This study was carried out according to the principles of the Declaration of Helsinki and the prevailing norms for performing investigation in humans. The use of this technology was approved by the institutional review boards. All human participants have provided signed informed consent.

2.6. Clinical data

Demographic, intraoperative, and postoperative data were obtained. Complications were classified according to the Clavien-Dindo classification [9].

2.7. Statistical analysis

Statistical analyses (Student t test) were performed to assess the concordance between the measures of the model with or without its plaques and the real vessels. IPSS software was employed to perform statistical analysis.

3. Results

A total of 19 patients were enrolled in this study. Five patients were considered in the feasibility group (F), ten in the accuracy group (A), and four in the efficacy group (E).

Demographic variables are reported in Table 1. The mean serum creatinine (sCr) levels in the F (6.53 mg/dl) and E (4.96 mg/dl) groups differ deeply from that in the A group (0.98 mg/dl) because these patients were not suffering from chronic kidney disease.

Intra- and postoperative data are shown in Table 2. The mean operative time in the transplantation groups (F: 168 min and E: 155 min) and in the prostatectomy group (A: 139 min) were comparable with the literature data available. No Clavien-Dindo ≥3 complications were recorded.

In the three groups, no differences were reported between vessel circumference size above the iliac bifurcation, at the level of the major plaque, and at the level of lacuna vasorum measured on the basis of the CT scan and 3D models (Table 3).

3.1. Feasibility group

The correspondence between 3D and CT circumference above the iliac bifurcation ($p = 0.36$) and at the level of lacuna vasorum ($p = 80.78$) is demonstrated in Table 3.

3.2. Accuracy group

The main characteristics of the iliac plaques are shown in Table 4. The mean longitudinal diameter (mm) of the plaques was 10.67 (standard deviation [SD] 8.06) and the mean transversal diameter was 4 (SD 3.55). The distance of the proximal edge of each plaque from the iliac bifurcation was reported. A US check of the position of the 3D plaques showed a discordance with 3D overlapping in 4/28 (14.29%) measures with a maximum of 3 mm error.

3.3. Efficacy group

In the third group (Table 5), the mean longitudinal diameter (mm) of the plaques was 11.66 (SD 8.02) and the mean transversal diameter was 4.5 (SD 2.64). A US check of the position of the 3D plaques showed a slight discordance with 3D overlapping in 3/14 (21.43%) measures, with a maximum of 3 mm error. In one of these patients, the inaccurate US-3D overlapping on the distal edge of the plaque led to an unsafe arteriotomy. In this case, due to the small amount of remaining atheromatic tissue, we decided to perform an arterial anastomosis instead of suturing the vessel and realizing a second arteriotomy. US-Doppler control was performed immediately after the procedure to confirm blood flow through the anastomosis, and it was repeated 1, 3, 24, and 48 h after the procedure, confirming the absence of thrombosis. The mean sCr at discharge was 1.97 mg/dl (SD 0.86).

In a median overall follow-up of 12 mo, no significant complications related to the specific surgical procedure were recorded.

4. Discussion

RAKT has been shown to be potentially the future of KT. This study represents the second step to overcome one of the main limitations of RAKT that was withholding the indication to a selected population.

In fact, multicentric prospective series from the European Association of Urology Robotic Urology Section Working Group have shown the safety and efficacy of the robotic technique in living donors and in autotransplantation [4], [5], [10].

Several advantages of this minimally invasive technique over the open approach were reported in selected population, such as in obese patients [11]. The feasibility of this technique in challenging settings, such as graft with multiple vessels, was also proved [12], and new technologies are on the way to improve surgical performance of the robotic approach in this field [13].

One of the main limitations of the robotic approach in the setting of KT is related to recipients with advanced atheromatic vascular disease, which may show multiple external iliac artery plaques, thus making the arterial clamping and arteriotomy challenging and unsafe. In fact, the first advantage of the open technique over the robotic approach in recipients with atherosclerotic vessels is constituted by the

availability of the haptic feedback that allows locating the plaques and avoiding them in order to safely perform the surgical steps of KT. The second advantage is represented by the possibility of relocating the clamps rapidly if the plaques prevented correct clamping of the artery. Those recipients are frequently candidate for receiving cadaveric donors' grafts and, at the moment, almost none of them is scheduled for robotic surgery.

To overcome this limit, 3D imaging reconstruction of the vessel with its plaques may be superimposed on the operative field through the AR showing the hidden anatomy of the atheromatic vessels.

By now, the 3D AR has mainly been employed in oncology to improve outcomes both in patient counseling and during the operation [14], [15], [16]. Its use in KT was conceived to expand the indication to RAKT in recipients of both living and deceased donors' grafts with arterial plaques.

Other techniques may be employed to locate the arterial plaques, for example, direct palpation of the vessel through a Pfannestiel incision, but this strategy may not be precise. Moreover, this technique cannot be used in case of a median incision, which is performed routinely in several centers [17].

In the IDEAL phase 1 of this project, our aim was to develop standardized steps to analyze the applicability of this technique providing a "proof of principle" of its efficacy. The inclusion of patients undergoing iliac-obturatory lymph node dissection allowed an initial assessment of the technique's accuracy in a safer setting of patients not undergoing vascular surgery. At the end of this proof of principle, the efficacy of the superimposition on real vessels was finally proved, leading to the first cases of 3D AR–guided RAKT.

Several technical and logistic difficulties were overcome during the development of the technique. First, different cohorts of patients were enrolled in the study prior to the start of the efficacy testing [8]. Second, more centers from different countries collaborated in the project. In addition, bioengineers with dedicated equipment have constantly worked beside the surgeons in the operative room during all the phases. From a technical point of view, the straight collaboration between surgeons with significant experience in 3D AR surgery and expert robotic transplantation surgeons allowed to overcome several difficulties related to the adaptation of the abovementioned technology in a new surgical setting.

Our study is not devoid of limitations. First of all, in one of the four patients who underwent 3D AR–guided RAKT, we observed a slightly inaccurate US-3D overlapping (max 3 mm) of the virtual plaque leading to an unsafe arteriotomy. Considering this experience, a 5 mm security distance over the virtual model's edges should always be respected. Moreover, we assumed that the arteriotomy might be performed on the surface of very small, poorly calcified, arterial plaques not clearly detectable by CT images and intraoperative US scan. This may also occur during an OKT due to the chance of missing a very small plaque by manual palpation.

Second, in this study, we considered a limited number of patients, respecting the first phase of the IDEAL [7]. Phase 2a will aim to show the reproducibility of the technique, enrolling a larger cohort of patients. In fact, this technology should be usable in a standardized fashion to achieve the awaited surgical results and to be safely reproduced in other centers. In order to expand the indication also to recipients of deceased donors' grafts, 3D virtual models have to be available in an urgency setting and should be usable as soon as a graft comes for transplantation.

This procedure may appear time consuming and thus in some cases not applicable. Actually, the overlapping procedures are performed during a surgical "spare time." In fact, the preparation of the living donor graft recipient is usually realized in advance while the donor's nephrectomy is being performed in another operative room.

At the moment, the cost of a 3D AR–guided RAKT, comprehensive of the development of the 3D virtual model and the availability of a dedicated rack to allow AR superimposition, has not yet been defined since

the study is still ongoing. Another current limitation is related to the reproducibility of this technique. For this reason, since the highly complex initial developmental steps were completed, we are designing a structured teaching program for 3D model superimposition to allow each surgeon to perform an accurate overlapping autonomously. Moreover, new strategies to automatically overlap the 3D virtual models using artificial intelligence are on the way to improve the precision of virtual model superimposition and to make the surgeon autonomous during the operation [18], [19].

5. Conclusions

The use of 3D AR in RAKT is a pioneering technique that has the potential to expand the indication to the robotic approach in patients with atheromatic plaques.

Funding/Support and role of the sponsor: None.

References

1. D.W. Johnson, K. Herzig, D. Purdie, et al. A comparison of the effects of dialysis and renal transplantation on the survival of older uremic patients. Transplantation, 69 (2000), pp. 794-799
2. R.A. Wolfe, V.B. Ashby, E.L. Milford, et al. Comparison of mortality in all patients on dialysis, patients on dialysis awaiting transplantation, and recipients of a first cadaveric transplant. N Engl J Med, 341 (1999), pp. 1725-1730
3. European Association of Urology. EAU guidelines on renal transplantation—Uroweb. https://uroweb.org/guidelines/renal-transplantation/summary-of-changes/2022.
4. M. Musquera, L. Peri, T. Ajami, et al. Robot-assisted kidney transplantation: update from the European Robotic Urology Section (ERUS) series. BJU Int, 127 (2021), pp. 222-228
5. Territo, L. Gausa, A. Alcaraz, et al. European experience of robot-assisted kidney transplantation: minimum of 1-year follow-up. BJU Int, 122 (2018), pp. 255-262
6. E. Checcucci, D. Amparore, C. Fiori, et al. 3D imaging applications for robotic urologic surgery: an ESUT YAUWP review. World J Urol, 38 (2020), pp. 869-881
7. P. McCulloch, D.G. Altman, W.B. Campbell, et al. No surgical innovation without evaluation: the IDEAL recommendations. Lancet, 374 (2009), pp. 1105-1112
8. Piana, A. Territo, A. Gallioli, et al. V02–01 New technologies in robot-assisted kidney transplantation: improving surgical performances, expanding the indication. J Urol, 206 (2021), p. e133
9. P.A. Clavien, J. Barkun, M.L. de Oliveira, et al. The Clavien-Dindo classification of surgical complications: five-year experience. Ann Surg, 250 (2009), pp. 187-196
10. Breda, P. Diana, A. Territo, et al. Intracorporeal versus extracorporeal robot-assisted kidney autotransplantation: experience of the ERUS RAKT Working Group. Eur Urol, 81 (2022), pp. 168-175
11. T. Prudhomme, J.B. Beauval, M. Lesourd, et al. Robotic-assisted kidney transplantation in obese recipients compared to non-obese recipients: the European experience. World J Urol, 39 (2021), pp. 1287-1298
12. S.A. Nataraj, F.A. Zafar, P. Ghosh, R. Ahlawat Feasibility and functional outcome of robotic assisted kidney transplantation using grafts with multiple vessels: comparison to propensity matched contemporary open kidney transplants cohort. Front Surg, 7 (2020), p. 51
13. Territo, A. Piana, M. Fontana, et al. Step-by-step development of a cold ischemia device for open and robotic-assisted renal transplantation. Eur Urol, 80 (2021), pp. 738-745

14. F. Porpiglia, E. Checcucci, D. Amparore, et al. Three-dimensional augmented reality robot-assisted partial nephrectomy in case of complex tumours (PADUA ≥10): a new intraoperative tool overcoming the ultrasound guidance. Eur Urol, 78 (2020), pp. 229-238
15. D. Amparore, F. Piramide, A. Pecoraro, et al. Identification of recurrent anatomical clusters using three-dimensional virtual models for complex renal tumors with an imperative indication for nephron-sparing surgery: new technological tools for driving decision-making. Eur Urol Open Sci, 38 (2022), pp. 60-66
16. F. Porpiglia, E. Checcucci, D. Amparore, et al. Three-dimensional elastic augmented-reality robot-assisted radical prostatectomy using hyperaccuracy three-dimensional reconstruction technology: a step further in the identification of capsular involvement Eur Urol, 76 (2019), pp. 505-514
17. M. Menon, A. Sood, M. Bhandari, et al. Robotic kidney transplantation with regional hypothermia: a step-by-step description of the Vattikuti Urology Institute-Medanta technique (IDEAL phase 2a). Eur Urol, 65 (2014), pp. 991-1000
18. D. Amparore, E. Checcucci, P. Piazzolla, et al. Indocyanine green drives computer vision based 3D augmented reality robot assisted partial nephrectomy: the beginning of “automatic” overlapping era. Urology, 164 (2022), pp. e312-e316
19. E. Checcucci, R. Autorino, G.E. Cacciamani, et al. Artificial intelligence and neural networks in urology: current clinical applications. Minerva Urol Nefrol, 72 (2020), pp. 49-57

Fig. 1

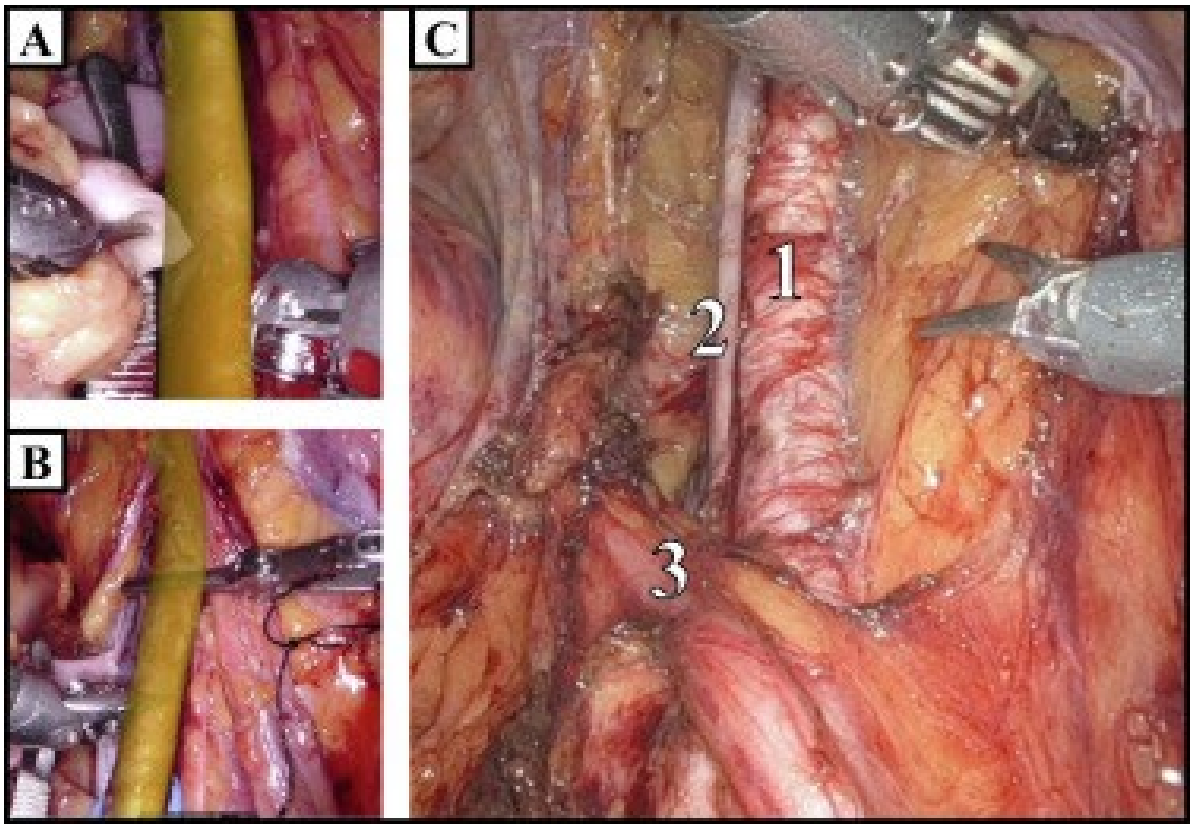

Feasibility assessment. (A) Preliminary tests of overlapping fidelity in a clinical case without arterial plaques: arteriotomy; (B) Preliminary tests of overlapping fidelity in a clinical case without arterial plaques: vascular clamping; (C) anatomical landmarks used to guide the 3D virtual model superimposition: 1—external iliac artery, 2—external iliac vein, and 3—right ureter. 3D = three dimensional.

Fig.2

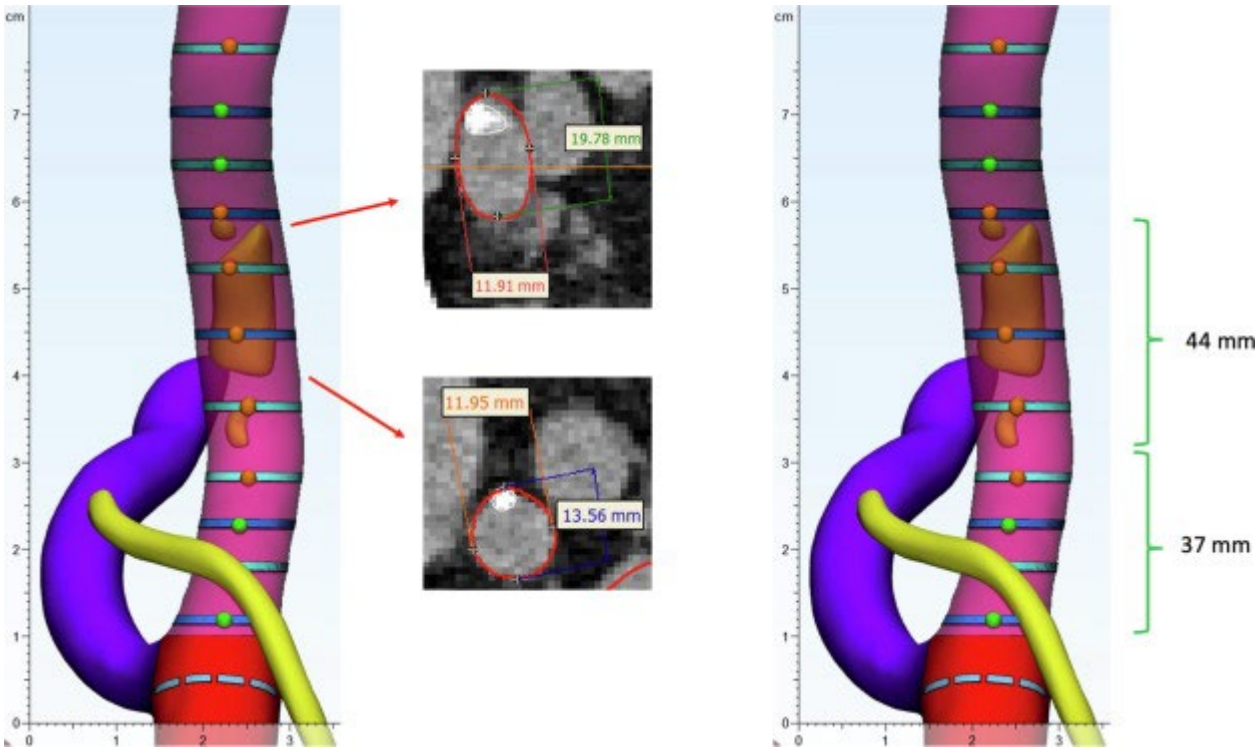

Accuracy assessment. Comparison between CT scan images and 3D virtual model circumference of the vessel above the iliac bifurcation, at the level of the major plaque and the level of lacuna vasorum. CT = computed tomography; 3D = three dimensional.

Fig.3

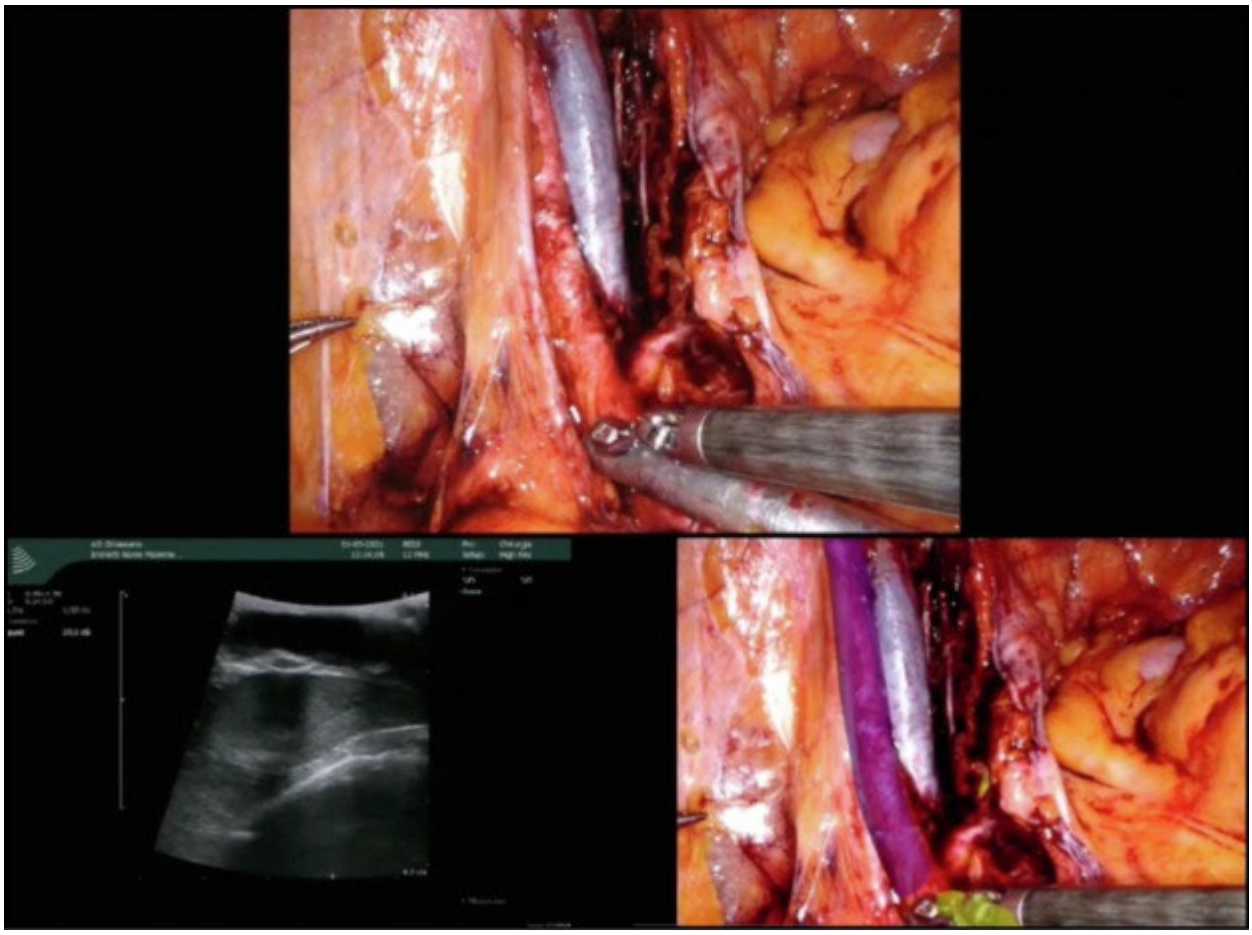

Accuracy assessment. US check of the position of the plaques showed on the 3D virtual models in patients undergoing pelvic lymph node dissection prior to robotic-assisted radical prostatectomy. 3D = three dimensional; US = ultrasound.

Fig. 4.

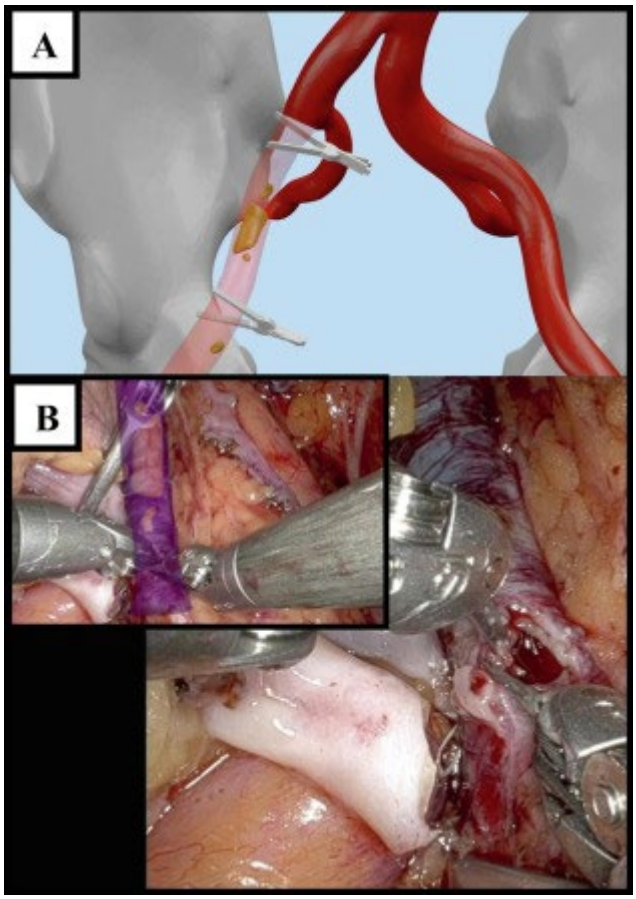

Efficacy assessment. (A) Preoperative vascular clamping strategy based on the 3D virtual reconstruction of the iliac arteries and plaques, and (B) 3D augmented reality–guided arteriotomy. 3D = three dimensional.

Table 1. Population demographics and preoperative features

	Feasibility group	Accuracy group	Efficacy group
Number of patients	5	10	4
Age (yr), mean (SD)	39 (16)	62 (7)	55
Gender, *n* (%)			
Male	5 (100)	10 (100)	3 (75)
Female	0 (0)	0 (0)	1 (25)
BMI (kg/m^2), mean (SD)	25.8 (4.76)	27.5 (3.97)	24.3 (2.75)
Preoperative sCr (mg/dl)	6.53 (4.08)	0.98 (0.62)	4.96 (0.33)
Postoperative sCr (mg/dl)	1.56 (0.92)	0.94 (0.55)	1.97 (0.86)
ASA score, median (IQR)	3 (2–3)	2 (1–3)	3 (3–3)
CCI age adjusted, median (IQR)	2 (0–2)	1 (0–2)	2 (1–3)

ASA=American Society of Anesthesiologists; BMI = body mass index; CCI = Charlson comorbidity index; IQR = interquartile range; sCr = serum creatinine; SD = standard deviation.

Table 2. Operative variables

	Feasibility group	Accuracy group	Efficacy group
Number of patient	5	10	4
EBL (cc), mean (SD)	180 (35)	236 (45)	155 (50)
Operative time (console) (min), mean (SD)	168 (43)	139 (38)	180 (29)
Transfusion rate, *n* (%)	0 (0)	0 (0)	0 (0)
Intraoperative complications, *n* (%)	0 (0)	0 (0)	1 (25)
Postoperative complications, *n* (%)	1 (20)	0 (0)	1 (25)
Postoperative complications Clavien-Dindo ≥3, *n* (%)	0 (0)	0 (0)	0 (0)
<90 POD readmission	0 (0)	0 (0)	0 (0)

EBL = estimated blood loss; POD = postoperative day; SD = standard deviation.

Table 3. Three-dimensional reconstruction CT scan concordance of the circumference measures of the vessels[a]

	Feasibility group (n = 5)		p value	Accuracy group (n = 10)		p value	Efficacy group (n = 4)		p value
	3D	CT		3D	CT		3D	CT	
C. 1 mm, mean (SD)	35.59 (3.72)	34.81 (3.65)	0.36	30.87 (4.42)	30.85 (4.41)	0.99	36.59 (5.6)	35.89 (5.3)	0.46
C. 2 mm, mean (SD)	NA[b]	NA[b]		33.93 (3.66)	34.1 (3.80)	0.75	34.92 (4.07)	34.92 (4.07)	1.00
C. 3 mm, mean (SD)	31.6 (4.25)	30.99 (4.30)	0.78	29.15 (3.56)	29.07 (3.58)	0.87	32.45 (3.96)	32.61 (4.01)	0.90

CT = computed tomography; 3D = three dimensional; NA = not assessable; SD = standard deviation.

a

Circumferences are reported at three different sections of the vessel: right above the common iliac bifurcation (C. 1), at the level of the major plaque (C. 2), and at the level of lacuna vasorum (C. 3).

b

In this group, only patients with no atheromatic plaques were enrolled.

Table 4. Three-dimensional US measure concordance assessment (plaque) in the accuracy group

	Plaque longitudinal diameter (mm)	Plaque transversal diameter (mm)	Distance from the iliac bifurcation (mm)	US check 1	US check 2	Error (mm)
Accuracy group (n = 10)						
Case 1	6	2.3	72	Yes	Yes	
Case 2						
Plaque 1	2.4	1.5	2	Yes	Yes	
Plaque 2	3.6	3.4	47	Yes	Yes	
Case 3	9	2	55	Yes	No	2
Case 4	5.3	3.1	9	Yes	Yes	
Case 5						
Plaque 1	12	5.3	0	Yes	Yes	
Plaque 2	9	4	10	Yes	Yes	
Plaque 3	17	6.8	24	Yes	Yes	
Case 6	2	1	32	No	No	2
Case 7	11	4.5	20	Yes	Yes	
Case 8						
Plaque 1	8.4	7.1	18	Yes	Yes	
Plaque 2	28	9	41	Yes	Yes	
Case 9	7.3	5.7	39	No	Yes	3
Case 10	2	1.5	21	Yes	Yes	

Distance = distance (mm) of the proximal edge of the plaque from the iliac bifurcation; 3D = three dimensional; US = ultrasound; US check 1 = concordance of the position of the 3D proximal edge of the plaque by using a US drop-in probe; US check 2 = concordance of the position of the 3D distal edge of the plaque; Error = measure (mm) of the discrepancy between the plaque's edge individuated on 3D virtual model overlapping and US probe sliding.

Table 5. Three-dimensional US measure concordance assessment (plaque) in the efficacy group

	Plaque longitudinal diameter (mm)	Plaque transversal diameter (mm)	Distance from the iliac bifurcation (mm)	US check 1	US check 2	Error (mm)	Safe clamping	Safe arteriotomy
Efficacy group (n = 4)								
Case 1	3.7	2	83	No	No	2	Yes	No
Case 2								
Plaque 1	9.5	5	39	No	Yes	3	Yes	Yes
Plaque 2	11	8	74	Yes	Yes			
Case 3	5.4	3		Yes	Yes		Yes	Yes
Case 4								
Plaque 1	6.1	2.6	37	Yes	Yes		Yes	Yes
Plaque 2	20	7.4	47	Yes	Yes		Yes	Yes
Plaque 3	4	3.1	68	Yes	Yes		Yes	Yes

3D = three dimensional; US = ultrasound; US check 1 = concordance of the position of the 3D proximal edge of the plaque by using a US drop-in probe; US check 2 = concordance of the position of the 3D distal edge of the plaque; Error = measure (mm) of the discrepancy between the plaque's edge individuated on 3D virtual model overlapping and US probe sliding.